An Efficient Method for Electromagnetic Characterization of 2-D Geometries in Stratified Media

M. I. Aksun, *Senior Member, IEEE*, F. Çalışkan, *Student Member, IEEE*, and Levent Gürel, *Senior Member, IEEE*

***Abstract*—A numerically efficient technique, based on the spectral-domain method of moments (MoM) in conjunction with the generalized pencil-of-functions (GPOF) method, is developed for the characterization of two-dimensional geometries in multilayer planar media. This approach provides an analytic expression for all the entries of the MoM matrix, explicitly including the indexes of the basis and testing functions provided that the Galerkin's MoM is employed. This feature facilitates an efficient modification of the geometry without the necessity of recalculating the additional elements in the MoM matrix. To assess the efficiency of the approach, the results and the matrix fill times are compared to those obtained with two other efficient methods, namely, the spatial-domain MoM in conjunction with the closed-form Green's functions, and a fast Fourier transform algorithm to evaluate the MoM matrix entries. Among these, the spectral-domain MoM using the GPOF algorithm is the most efficient approach for printed multilayer geometries.**

I. Introduction

ADVANCES in high-speed digital computers have led to the development of more sophisticated numerical methods to solve large electromagnetic problems of practical interest, which, by classical techniques, would be virtually impossible. Common numerical techniques that are used in electromagnetic problems are the method of moments (MoM) [1], [2], finite-element methods (FEMs) [3], and the finite-difference time-domain (FDTD) methods [4], all of which basically transform integral, differential, or integro-differential equations into algebraic equations. Therefore, the computational efficiency of these techniques is dependent on the efficiency of forming a set of linear equations and on the number of unknowns. Among these techniques, the MoM plays an important role for the solution of open field problems, particularly for printed geometries in planar stratified media.

Recently, for two-dimensional (2-D) geometries, there has been several interesting studies to characterize scattering and propagation nature of printed strip and slot structures in layered environment [5]–[10]. In this paper, two new MoM-based approaches are developed for 2-D planar geometries, and compared to the most efficient approach available in the literature, namely, the MoM using a fast Fourier transform (FFT) algorithm. These new approaches are based on the MoM; one employs the closed-form Green's functions of 2-D planar geometries in the spatial domain and the other uses the generalized pencil-of-functions (GPOF) method in conjunction with the spectral-domain MoM. It is observed that the spectral-domain MoM with the GPOF method performs the best as far as the efficiencies of the methods are concerned, of course, with the same level of accuracy in all approaches.

The first step of the MoM formulation is to write an integral equation describing the electromagnetic problem, which could be the mixed potential integral equation (MPIE) or the electric-field integral equation (EFIE) for the printed geometries [11]. These integral equations require related Green's functions, either of the vector and scalar potentials (for MPIE formulation) or of the electric fields (for EFIE formulation). Since the spectral-domain Green's functions for planar geometries are available in closed form, their spatial-domain counterparts are obtained via an efficient inverse Fourier transform algorithm. Once the spatial-domain Green's functions are obtained, the solution due to a general source in 2-D can be obtained by the principle of linear superposition. The next step in the MoM formulation is to expand the unknown function in terms of known basis functions with unknown coefficients. The boundary conditions are then implemented in an integral sense through the testing procedure. Following these steps, the integral equation is transformed to a matrix equation, whose entries are double integrals for general 2-D geometries; one for the convolution integral to find the electric field, and one for the testing procedure to apply the boundary condition. However, for planar 2-D geometries, the MoM matrix entries can be reduced to single integrals by transforming the convolution integrals onto the basis and testing functions and by evaluating the resulting integrals analytically [12]. In the spectral-domain application of the MoM, since the Green's functions are known in closed form, the matrix entries become single integrals over an infinite domain. Consequently, in either domain, the computational efficiency of the MoM lies in the evaluation of the MoM matrix entries, of course, for moderate-size geometries. For a geometry requiring a large number of unknowns, the matrix solution time dominates the overall performance of the technique, therefore, the efficiency of the method is defined by the efficiency of the linear system solver [13].

Recently, for the characterization of two-and-one-half-dimensional (2.5-D) microstrip structures, the spatial-domain

Manuscript received February 6, 2001; revised May 15, 2001.

M. I. Aksun was with the Department of Electrical and Electronics Engineering, Bilkent University, 06533 Ankara, Turkey. He is now with the Department of Electrical and Electronics Engineering, Koç University, 80910 Istanbul, Turkey.

F. Çalışkan was with the Department of Electrical and Electronics Engineering, Bilkent University, 06533 Ankara, Turkey. She is now with the School of Electrical and Computer Engineering, Georgia Institute of Technology, Atlanta, GA 30332-0250 USA.

L. Gürel is with the Department of Electrical and Electronics Engineering, Bilkent University, 06533 Ankara, Turkey.

Publisher Item Identifier S 0018-9480(02)04069-3.

MoM has become the most efficient tool because of the availability of an efficient algorithm for the derivation of the closed-form spatial-domain Green's functions [14]–[20]. With this in mind, we have first derived the closed-form approximations of the Green's functions for 2-D geometries as a finite sum of the Hankel functions. The MoM matrix entries, which are single integrals over finite domains, are then evaluated numerically, thinking that the spatial-domain MoM in conjunction with the closed-form Green's functions would be more efficient than the spectral-domain MoM in conjunction with the FFT algorithm. However, this approach has become computationally more expensive than the MoM using the FFT algorithm for the evaluation of the matrix entries. This is mainly due to the fact that the latter approach calculates all the entries of the MoM matrix at once, while the former calculates the entries one by one. While formulating the spectral-domain MoM, we have recognized that the computational efficiency of the evaluation of the MoM matrix entries can be significantly improved by using the GPOF method instead of the FFT algorithm [21]. This new approach not only improves the efficiency of obtaining the MoM matrix, but also provides only one closed-form expression for all the entries of the MoM matrix, explicitly including the indexes of the basis and testing functions. Hence, one can easily extend the geometry, for which the same analytical expression is valid for the MoM matrix entries, without calculating the MoM matrix entries corresponding to the modified portion of the original geometry. Therefore, the contribution of this paper is to introduce the following two new approaches for the calculation of the MoM matrix in 2-D geometries: 1) the spatial-domain MoM in conjunction with the closed-form Green's functions and 2) the spectral-domain MoM with the GPOF method. In addition, these approaches are compared to a well-known efficient approach for 2-D geometries, namely, the spectral-domain MoM with an FFT algorithm. It is observed that the most efficient one is the proposed spectral-domain MoM using the GPOF algorithm.

The derivation of the closed-form Green's functions in 2-D planar geometries is briefly introduced and a typical set of Green's functions are demonstrated in Section II. The use of these closed-form Green's functions in the spatial-domain MoM is then discussed for computational efficiency, and the new spectral-domain MoM using the GPOF method is developed in Section III. Also included in Section III, for the sake of comparison, is a brief description of the well-known spectral-domain MoM using an FFT algorithm. In Section IV, numerical examples and comparisons for the computational efficiency of the aforementioned three methods are included, which is followed by a conclusion in Section V.

II. Closed-Form Green's Functions for 2-D Planar Geometries

For the sake of illustration, consider a planar multilayer medium shown in Fig. 1, where it is assumed that the layers extend to infinity in the transverse directions. A line source, extended to infinity in the y-direction and polarized either in the y- or x-directions, is embedded in region-i and the observation point can be in any arbitrary layer. Each layer can

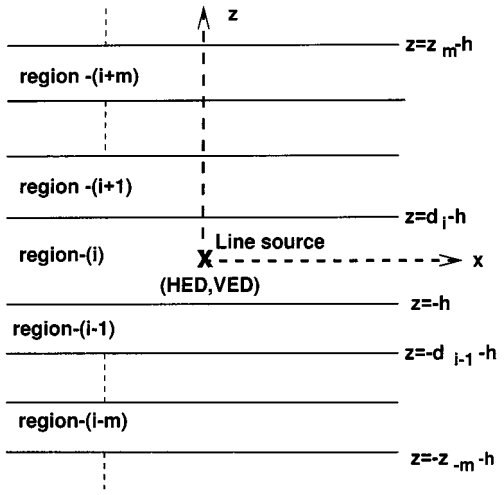

Fig. 1. Line source embedded in a multilayer medium.

have different electric and magnetic properties (ϵ_{r_i}, μ_{r_i}) and thickness (d_i) and, moreover, perfect electric conducting planes and half-spaces are also regarded as layers in this formulation.

The first step in the derivation of the spatial-domain Green's functions is to obtain the closed-form representations of the spectral-domain Green's functions. The derivation of the spectral-domain Green's functions for a dipole source in planar media has been given in [22] and [23], and the closed-form expressions for the Green's functions have been provided in [17]. For the case of a line source extending to infinity in the y-direction, the closed-form expressions obtained for the dipole cases are still valid with a difference in the definition of the dispersion relation, i.e., $k_i^2 = k_x^2 + k_y^2 + k_{z_i}^2$ of a dipole should be replaced by $k_i^2 = k_x^2 + k_{z_i}^2$ for a line source. This is because the fields are invariant in the y-direction for a line source extending to infinity in the y-direction in a planar multilayer medium. In other words, we can use the same spectral-domain Green's functions for a line source as those for dipoles, provided $k_{z_i} = \sqrt{k_i^2 - k_x^2}$ is used. For the sake of completeness, the components of the Green's functions that are to be used in the following sections are given in the following source layer:

$$\tilde{G}_{yy}^A = \frac{\mu_i}{2jk_{z_i}} \left\{ e^{-jk_{z_i}|z|} + A_h^e e^{jk_{z_i}z} + C_h^e e^{-jk_{z_i}z} \right\} \tag{1}$$

for a line source $\overline{\mathbf{J}} = \hat{\mathbf{y}}\delta(\rho)$

$$\tilde{G}_{xx}^A = \tilde{G}_{yy}^A \tag{2}$$

$$\tilde{G}_x^{q_e} = \frac{1}{j2\epsilon_i k_{z_i}} \left\{ e^{-jk_{z_i}|z|} + \frac{k_{z_i}^2 B_h^e + k_i^2 A_h^e}{k_x^2} e^{jk_{z_i}z} + \frac{k_i^2 C_h^e - k_{z_i}^2 D_h^e}{k_x^2} e^{-jk_{z_i}z} \right\} \tag{3}$$

for a line source $\overline{\mathbf{J}} = \hat{\mathbf{x}}\delta(\rho)$, where the coefficients A_h^e, B_h^e, C_h^e, and D_h^e are functions of the generalized reflection coefficients $\tilde{R}_{\mathrm{TE,\,TM}}$ given in [17], and $\sim$ over the Green's functions and the field components denotes the spectral-domain representation. The other components of the spectral-domain Green's functions in the source layer and the coefficients used in these expressions

can be found in [17], and the field expressions in any other layer can be obtained iteratively, as described in [17] and [22].

Once the spectral-domain Green's functions are obtained as in (1)–(3), their spatial-domain counterparts are calculated by taking the inverse Fourier transform, which is defined as

$$G^{A,\,q_e} = \frac{1}{2\pi}\int_{-\infty}^{\infty} dk_x e^{-jk_x x}\tilde{G}^{A,\,q_e} \tag{4}$$

where G and $\tilde{G}$ are the Green's functions in the spatial and spectral domains, respectively. Note that this transformation cannot be evaluated analytically, except for a few special cases. Therefore, it requires a numerical integration algorithm, resulting in a very time-consuming process for the calculation of the spatial-domain Green's functions. However, if the spectral-domain Green's functions (apart from $1/k_{z_i}$ terms) can be approximated in terms of complex exponentials, the analytical evaluation of the Fourier transform integral (4) becomes possible via the following integral identity [22]:

$$H_0^{(2)}(k_\rho\rho) = \frac{1}{\pi}\int_{-\infty}^{\infty}\frac{e^{-jk_x x - jk_z|z|}}{k_z}\,dk_x. \tag{5}$$

Therefore, the crucial step in the derivation of the closed-form spatial-domain Green's functions is the exponential approximation of the spectral-domain Green's functions. Since the exponential approximation technique (i.e., GPOF) together with the two-level approach (to sample the function to be approximated along the integration path) is detailed and applied to the Hankel transformation of the spectral-domain Green's functions for a dipole source in a stratified medium in [24], it is not given here for the sake of brevity. Instead, the procedure to obtain the closed-form Green's functions starting from the spectral-domain representations is given here for a typical Green's function G_{yy}^A. Note that the spectral-domain Green's functions are obtained as referenced to Fig. 1, where the origin of the coordinate system is at the source location. However, for the application of the MoM, the origin is set to the bottom of the source layer, then h and z are replaced in all spectral-domain Green's functions by z' and $z-z'$, respectively. Hence, the Green's functions would be the explicit functions of z and z'. The steps of getting the spatial-domain Green's functions, with explicit z and z' variables, are given as follows.

- Write the spectral-domain representation of G_{yy}^A in terms of exponentials of z and z' as

$$\begin{aligned}\tilde{G}_{yy}^A = \frac{\mu_i}{j2k_{z_i}}\Big(&e^{-jk_{z_i}|z-z'|} + \tilde{R}_{\rm TE}^{i,i+1}M_i^{\rm TE}e^{-jk_{z_i}2d_i}e^{jk_{z_i}(z+z')}\\ &+\tilde{R}_{\rm TE}^{i,i-1}\tilde{R}_{\rm TE}^{i,i+1}M_i^{\rm TE}e^{-jk_{z_i}2d_i}e^{jk_{z_i}(z-z')}\\ &+\tilde{R}_{\rm TE}^{i,i-1}M_i^{\rm TE}e^{-jk_{z_i}(z+z')}\\ &+\tilde{R}_{\rm TE}^{i,i-1}\tilde{R}_{\rm TE}^{i,i+1}M_i^{\rm TE}e^{-jk_{z_i}2d_i}e^{-jk_{z_i}(z-z')}\Big).\end{aligned} \tag{6}$$

- Approximate the coefficients in (6) by the complex exponentials of k_{z_i} via the GPOF method and two-level sampling approach [24]

$$\begin{aligned}\tilde{G}_{yy}^A = \frac{\mu_i}{j2k_{z_i}}\Bigg\{&e^{-jk_{z_i}|z-z'|}\\ &+\sum_{n_{1yy}=1}^{N_{1yy}}C_{n_{1yy}}e^{-\alpha_{n_{1yy}}k_{z_i}}e^{jk_{z_i}(z+z')}\\ &+\sum_{n_{2yy}=1}^{N_{2yy}}C_{n_{2yy}}e^{-\alpha_{n_{2yy}}k_{z_i}}e^{jk_{z_i}(z-z')}\\ &+\sum_{n_{3yy}=1}^{N_{3yy}}C_{n_{3yy}}e^{-\alpha_{n_{3yy}}k_{z_i}}e^{-jk_{z_i}(z+z')}\\ &+\sum_{n_{2yy}=1}^{N_{2yy}}C_{n_{2yy}}e^{-\alpha_{n_{2yy}}k_{z_i}}e^{-jk_{z_i}(z-z')}\Bigg\}\end{aligned} \tag{7}$$

where $C_{n_{iyy}}$ and $\alpha_{n_{iyy}}(i=1,\,2,\,3)$ are the complex coefficients and exponents of the complex exponentials, respectively, approximating the three terms in (6).

- Take the inverse Fourier transform of the spectral-domain Green's function $\tilde{G}_{yy}^A$ analytically using the integral identity given in (5)

$$\begin{aligned}G_{yy}^A = -\frac{j\mu_i}{4}\Bigg\{&H_0^{(2)}(k_i\rho)+\sum_{n_{1yy}=1}^{N_{1yy}}C_{n_{1yy}}H_0^{(2)}\left(k_i\rho_{n_{1yy}}\right)\\ &+\sum_{n_{2yy}=1}^{N_{2yy}}C_{n_{2yy}}H_0^{(2)}\left(k_i\rho_{n_{2yy}}^{(1)}\right)\\ &+\sum_{n_{3yy}=1}^{N_{3yy}}C_{n_{3yy}}H_0^{(2)}\left(k_i\rho_{n_{3yy}}\right)\\ &+\sum_{n_{2yy}=1}^{N_{2yy}}C_{n_{2yy}}H_0^{(2)}\left(k_i\rho_{n_{2yy}}^{(2)}\right)\Bigg\}\end{aligned} \tag{8}$$

where

$$\begin{aligned}\rho &= \sqrt{(x-x')^2+(z-z')^2}\\ \rho_{n_{1yy}} &= \sqrt{(x-x')^2+\left(z+z'+j\alpha_{n_{1yy}}\right)^2}\\ \rho_{n_{2yy}}^{(1)} &= \sqrt{(x-x')^2+\left(z-z'+j\alpha_{n_{2yy}}\right)^2}\\ \rho_{n_{2yy}}^{(2)} &= \sqrt{(x-x')^2+\left(z-z'-j\alpha_{n_{2yy}}\right)^2}\\ \rho_{n_{3yy}} &= \sqrt{(x-x')^2+\left(z+z'-j\alpha_{n_{3yy}}\right)^2}\end{aligned}$$

which are mostly complex numbers and, therefore, their branches must be chosen such that the zeroth-order Hankel function of the second kind should be a decaying function for large values of arguments. Note that G_{xx}^A is equal to G_{yy}^A, and the other components of the Green's functions can be obtained in closed forms following the same procedure.

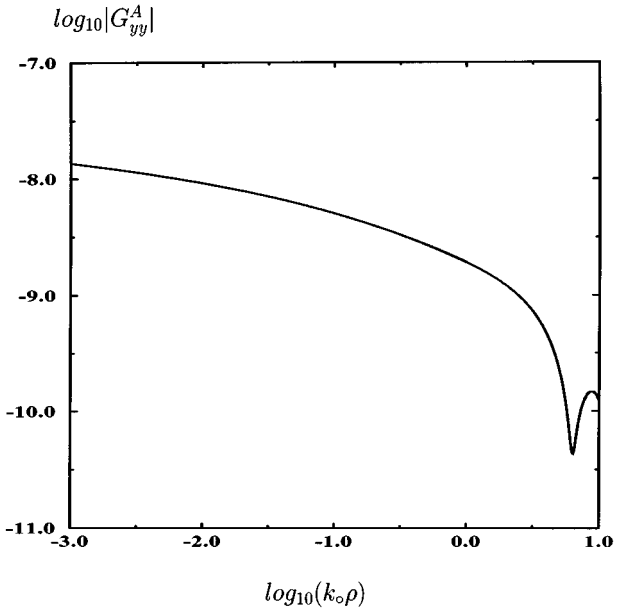

Fig. 2. Magnitude of the Green's function for the vector potential G^A_{yy}. A two-layer medium: $\epsilon_{r_{i-1}} = 4.0$, $\epsilon_{r_i} = 1.0$, $z = z' = 0$.

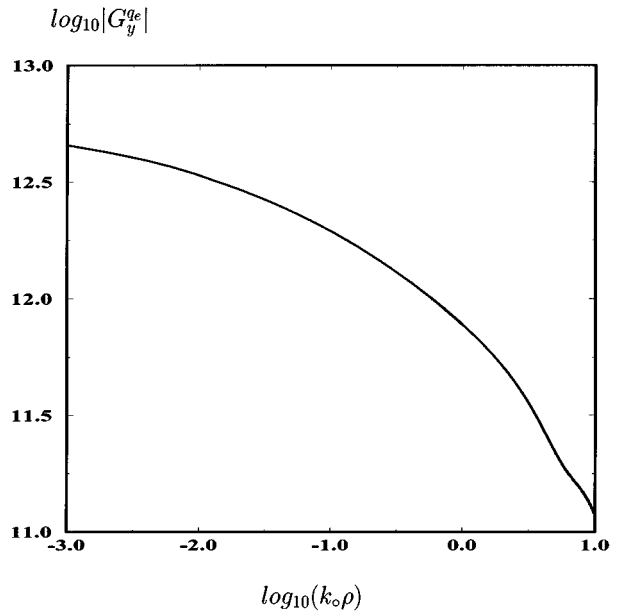

Fig. 3. Magnitude of the Green's function for the scalar potential G^q_y. A two-layer medium: $\epsilon_{r_{i-1}} = 4.0$, $\epsilon_{r_i} = 1.0$, $z = z' = 0$.

To give an idea as to how these closed-form Green's functions behave, an example is provided for a two-layer medium: the first layer has a relative permittivity of four and the second layer is free space, the source is placed at the interface and, hence, $z = z' = 0$. The plots of the Green's functions G^A_{yy} and $G^{q_e}_y$ are given in Figs. 2 and 3.

III. Formulations of 2-D Problems via MoM

The first step in the application of any form of the MoM is to derive an operator equation, i.e., integral equation for this study, that would describe the problem mathematically. Therefore, before giving the details of the application of the MoM,

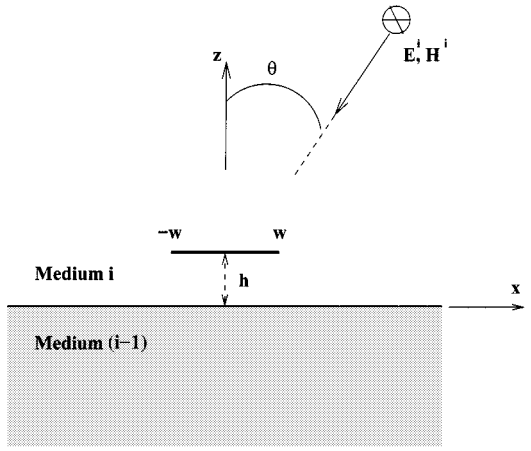

Fig. 4. Typical strip geometry in two semiinfinite half-spaces with a plane-wave illumination.

the scattered electric fields from a typical 2-D planar geometry ($\partial/\partial y = 0$), as given in Fig. 4, are written as

$$E^s_x = -j\omega G^A_{xx} * J_x + \frac{1}{j\omega}\frac{\partial}{\partial x}\left[G^{q_e}_x * \frac{\partial}{\partial x} J_x + G^{q_e}_z * \frac{\partial}{\partial z} J_z\right] \tag{9}$$

$$E^s_y = -j\omega G^A_{yy} * J_y \tag{10}$$

$$E^s_z = -j\omega\left(G^A_{zx} * J_x + G^A_{zy} * J_y + G^A_{zz} * J_z\right) + \frac{1}{j\omega}\frac{\partial}{\partial z}\left[G^{q_e}_x * \frac{\partial}{\partial x} J_x + G^{q_e}_z * \frac{\partial}{\partial z} J_z\right] \tag{11}$$

where the superscript s denotes the scattered fields, and the current densities J_x, J_y, and J_z are the unknowns to be determined. Hence, the integral equation can be obtained by requiring that the tangential components of the total electric field ($\mathbf{E^s} + \mathbf{E^i}$) on conducting surfaces are to be zero. The incident electric fields for TE and TM to y polarizations are given, respectively, as follows:

$$\boldsymbol{E^i_{te}} = \frac{1}{w\epsilon_i} H_i \left((-\hat{x}k_z + \hat{z}k_x)e^{j(k_x x + k_z z)} + (\hat{x}k_z + \hat{z}k_x)\tilde{R}^{i,i-1}_{\mathrm{TM}} e^{j(k_x x - k_z z)}\right) \tag{12}$$

$$\boldsymbol{E^i_{tm}} = \hat{y}E_i \left(e^{j(k_x x + k_z z)} + \tilde{R}^{i,i-1}_{\mathrm{TE}} e^{j(k_x x - k_z z)}\right) \tag{13}$$

where $k_i = \sqrt{k_x^2 + k_z^2}$, $k_x = k_i \sin\theta$, and $k_z = k_i \cos\theta$. Note that we have used $\tilde{R}^{i,i-1}_{\mathrm{TM}}$ and $\tilde{R}^{i,i-1}_{\mathrm{TE}}$ in the expressions of the incident fields for TE to y and TM to y, respectively. This is because, in the derivation of the spectral-domain Green's functions where we have defined these generalized reflection coefficients, TE and TM are defined with respect to the z-direction.

Note that, for the discussion in this section, 2-D geometries are considered to be printed on the x–y-plane and, hence, no z-directed current exists, as given in Fig. 4. In other words, the only unknown is J_y for TM to y excitation and J_x for TE to y excitation. In the application of the MoM, after having obtained the governing integral equation, the unknown functions are expended in terms of known basis functions with unknown coefficients. Throughout this study, triangular functions and pulse

functions are chosen as the basis functions for J_x and J_y, respectively,

$$B_{xn}(x) = \begin{cases} 1 - \dfrac{|x - nh_x|}{h_x}, \\ \qquad \text{if } (n-1)h_x \le x \le (n+1)h_x \\ 0, \qquad \text{otherwise} \end{cases} \tag{14}$$

$$B_{yn}(x) = \begin{cases} 1, & \text{if } (n-1/2)h_x \le x \le (n+1/2)h_x \\ 0, & \text{otherwise.} \end{cases} \tag{15}$$

Since, in this study, both the spectral- and spatial-domain MoMs are employed, the spectral-domain representations of both basis functions and the incident field expressions are given here for the sake of completeness. The spectral-domain representations of the basis functions are as follows:

$$\tilde{B}_{xn}(k_x) = h_x e^{jk_x nh_x} \operatorname{sinc}^2\left(\frac{k_x h_x}{2}\right) \tag{16}$$

$$\tilde{B}_{yn}(k_x) = h_x e^{jk_x nh_x} \operatorname{sinc}\left(\frac{k_x h_x}{2}\right) \tag{17}$$

and the incident field expressions (tangential components only) are as follows:

$$\tilde{E}_x^i = -\frac{k_i \cos\theta H_i}{\omega \epsilon_i} 2\pi\delta(k_x + k_i \sin\theta) \cdot \left(e^{jk_i \cos\theta z} - \tilde{R}_{\mathrm{TM}}^{i,i-1} e^{-jk_i \cos\theta z}\right) \tag{18}$$

$$\tilde{E}_y^i = E_i 2\pi\delta(k_x + k_i \sin\theta) \cdot \left(e^{jk_i \cos\theta z} + \tilde{R}_{\mathrm{TE}}^{i,i-1} e^{-jk_i \cos\theta z}\right). \tag{19}$$

A. MoM Formulation in the Spatial Domain

Writing the total electric field as the sum of the scattered and incident electric fields, and implementing the boundary conditions for the tangential components on the conducting body result in the following electric-field integral equations:

$$(\hat{x}E_x^s)_{\tan} = -(\boldsymbol{E}_{te}^i)_{\tan} \text{ for TE excitation} \tag{20}$$

$$(\hat{y}E_y^s)_{\tan} = -(\boldsymbol{E}_{tm}^i)_{\tan} \text{ for TM excitation.} \tag{21}$$

With the application of the testing procedure of the MoM to these integral equations, the following algebraic equations are obtained:

$$\langle T_{xm}(x),\, E_x^s \rangle = -\langle T_{xm}(x),\, \hat{x} \cdot \boldsymbol{E}_{te}^i \rangle \text{ for TE excitation} \tag{22}$$

$$\langle T_{ym}(x),\, E_y^s \rangle = -\langle T_{ym}(x),\, \hat{y} \cdot \boldsymbol{E}_{tm}^i \rangle \text{ for TM excitation} \tag{23}$$

where $m = 1$ to N (= the number of basis functions) and the unknown current densities in the expressions of the scattered electric fields [see (9)–(11)] have already been written in terms of known basis functions $B_{(x,\,y)n}$ with unknown coefficients $I_{(x,\,y)n}$. Since the right-hand sides of (22) and (23) are simple to evaluate, the left-hand sides are written for each m as

$$\langle T_{xm}(x)\, E_x^s \rangle = -jw \sum_{n=1}^{N_{te}} I_{xn} \left\{ \left[\int dx T_{xm}(x) \left(G_{xx}^A * B_{xn}(x)\right) \right] - \frac{1}{\omega^2} \left[\int dx \frac{dT_{xm}(x)}{dx} \cdot \left(G_x^{q_e} * \frac{dB_{xn}(x)}{dx} \right) \right] \right\} \tag{24}$$

$$\langle T_{ym}(x),\, E_y^s \rangle = -jw \sum_{n=1}^{N_{tm}} I_{yn} \int dx T_{ym}(x) \left(G_{yy}^A * B_{yn}(x)\right) \tag{25}$$

for TE and TM excitations, respectively, where integration by parts is used for TE excitation to transfer the derivative onto the testing function [25]. The convolution integrals over the Green's functions and basis functions can be easily transformed onto the basis and testing functions and can then be evaluated analytically. As a result, a typical MoM matrix entry becomes a single integral of the Green's function multiplied with the analytical expression for the correlation of the basis and testing functions [12]. Since the Green's functions in the spatial domain are approximated as the sum of Hankel functions of the second kind, as in (8), they grow indefinitely for small arguments, and subsequently the integrals cannot be calculated efficiently. To perform a fair comparison among the MoM in the spatial and spectral domains, one needs to apply all the available tools to make the methods as efficient as possible. Therefore, to circumvent this inefficiency in the spatial-domain MoM, a singularity extraction method is employed for small arguments.

With the use of the closed-form Green's functions, and the singularity extraction method for the evaluation of the integrals [see (24) and (25)], the efficiency of the evaluation of these integrals is significantly improved. However, although this improvement is significant for each entry of the MoM matrix, it is not sufficient when it is compared to the efficiency of a technique calculating the entire MoM matrix in one step, like the FFT-based MoM.

B. MoM Formulation in the Spectral Domain

The scattered electric fields for TE and TM excitations can be rewritten in the spectral domain from (9) and (10) for a planar geometry (printed on the x–y-plane) as

$$\tilde{E}_x^s = -j\omega \tilde{G}_{xx}^E \tilde{J}_x(k_x) \tag{26}$$

$$\tilde{E}_y^s = -j\omega \tilde{G}_{yy}^A \tilde{J}_y(k_x) \tag{27}$$

where

$$\tilde{G}_{xx}^E = \tilde{G}_{xx}^A - \frac{k_x^2}{\omega^2} \tilde{G}_x^{q_e}$$

and $\tilde{G}_{xx}^E$ represents the spectral-domain Green's function for the x component of the electric field due to the x component of the electric current density. Expanding the unknown current

densities in terms of known basis functions and implementing the boundary conditions on the total electric field through the testing procedure of the MoM, the following set of linear equations are obtained:

$$-jw\sum_{n=1}^{N_{te}} I_{xn}\left\langle \tilde{T}^*_{xm},\, \tilde{G}^E_{xx}\tilde{B}_{xn}\right\rangle = -\left\langle \tilde{T}^*_{xm},\, \tilde{E}^i_x\right\rangle, \quad \text{for } m=1,\ldots,N_{te} \tag{28}$$

for TE excitation and

$$-jw\sum_{n=1}^{N_{tm}} I_{yn}\left\langle \tilde{T}^*_{ym},\, \tilde{G}^A_{yy}\tilde{B}_{yn}\right\rangle = -\left\langle \tilde{T}^*_{ym},\, \tilde{E}^i_y\right\rangle, \quad \text{for } m=1,\ldots,N_{tm} \tag{29}$$

for TM excitation. Note that all quantities, such as the basis and testing functions, Green's functions, and incident electric fields, are in the spectral domain. Contrary to the spatial-domain MoM, the Green's functions employed here are in closed forms already [see (1)–(3)]. Due to the definition of the inner product, the matrix entries are single integrals over an infinite domain, and are given with the basis and testing functions substituted as

$$\left\langle \tilde{T}^*_{xm},\, \tilde{G}^E_{xx}\tilde{B}_{xn}\right\rangle = \int_{-\infty}^{\infty} dk_x e^{-jk_x h_x(m-n)} h_x^2 \operatorname{sinc}^4\left(\frac{k_x h_x}{2}\right)\tilde{G}^E_{xx} \tag{30}$$

$$\left\langle \tilde{T}^*_{xm},\, \tilde{E}^i_x\right\rangle = -\frac{k_i\cos\theta H_i}{\omega\epsilon_i}\, 2\pi e^{j(k_i\sin\theta)mh_x} \times\left(e^{jk_i\cos\theta z} - \tilde{R}^{i,\,i-1}_{\mathrm{TM}} e^{-jk_i\cos\theta z}\right) \times h_x \operatorname{sinc}^2\left(\frac{(k_i\sin\theta)h_x}{2}\right) \tag{31}$$

for TE excitation and

$$\left\langle \tilde{T}^*_{ym},\, \tilde{G}^A_{yy}\tilde{B}_{yn}\right\rangle = \int_{-\infty}^{\infty} dk_x e^{-jk_x h_x(m-n)} h_x^2 \operatorname{sinc}^2\left(\frac{k_x h_x}{2}\right)\tilde{G}^A_{yy} \tag{32}$$

$$\left\langle \tilde{T}^*_{ym},\, \tilde{E}^i_y\right\rangle = E_i 2\pi e^{j(k_i\sin\theta)mh_x}\left(e^{jk_i\cos\theta z} + \tilde{R}^{i,\,i-1}_{\mathrm{TE}} e^{-jk_i\cos\theta z}\right) \times h_x \operatorname{sinc}\left(\frac{(k_i\sin\theta)h_x}{2}\right) \tag{33}$$

for TM excitation. If these terms were to be evaluated numerically for each m and n, the spectral-domain approach would have been very expensive computationally when compared to the spatial-domain MoM using the closed-form Green's functions. This is because the domain of integration is infinite, and the integrands are oscillatory functions. Instead of employing a quadrature algorithm for evaluating these integrals, one may try to get an analytic expression for the value of each integral or to employ a numerical technique that would yield the whole set of the MoM matrix entries.

1) Evaluation of MoM Matrix Entries With the FFT Method: As was stated in the previous section, the ultimate goal is to get the unknown coefficients I_{xn} and I_{yn} of the current densities efficiently from the solution of the matrix equations given in (28) and (29). This goal translates into the efficient evaluation of the matrix entries given explicitly in (30) and (32) due to the fact that the most time-consuming step in the spectral-domain MoM algorithm is the evaluation of these entries, at least for a moderate number of unknowns. This is mainly because each entry of the matrix equation is a single integral of complex oscillatory functions over an infinite domain, and because there is no analytical expression for the results of these integrals. However, using the fact that these integrals look like the Fourier transform integrals, an FFT-based algorithm can be employed to evaluate these integrals very efficiently. In this section, this approach is briefly outlined for the sake of assessing the efficiency of this algorithm and getting some intuition for the comparison with other two approaches; namely, the spatial-domain MoM using the closed-form Greens functions and the spectral-domain MoM using the GPOF method. The application of this FFT-based algorithm for the evaluation of the integrals [see (30) and (32)] is explained for a strip with a longitudinal direction in the y-axis and located on the x–y-plane, requiring only the incident field in the x-direction for TE excitation and in the y-direction for TM excitation. For the sake of brevity, only the case for TE excitation is given here in detail, as it is similar for TM excitation.

If the matrix entries in (30) are examined, it is seen that the exponential term acts as the kernel of the transformation, and the rest is the function to be transformed; hence, the function to be transformed is

$$F(k_x) = \operatorname{sinc}^4\left(\frac{k_x h_x}{2}\right)\tilde{G}^E_{xx} \tag{34}$$

where k_x is limited between $-K$ and K. Therefore, the matrix entries can be rewritten as

$$\left\langle \tilde{T}^*_{xm},\, \tilde{G}^E_{xx}\tilde{B}_{xn}\right\rangle = h_x^2\int_{-K}^{K} dk_x e^{-jk_x d}F(k_x) = I(d) \tag{35}$$

where $d=(m-n)h_x$ is used to denote the distance between the basis and testing functions. With a simple transformation of variable, this integral can be cast into the form of

$$\begin{aligned} I(d) &= h_x^2 e^{jKd}\int_0^{2K} dk'_x e^{-jk'_x d}F(k'_x - K) \\ &= h_x^2 e^{jKd}\sum_{r=1}^{R} F\left(k'_{x_r} - K\right)e^{-jk'_{x_r}d}\Delta \end{aligned} \tag{36}$$

where $k'_{x_r} = (r-1)\Delta$ and $\Delta = 2K/R$. Following this representation, an FFT routine (DFFTCF) from the International Mathematical and Statistical Libraries (IMSL) is used to compute the discrete complex Fourier transform of a complex vector

of size R. Specifically, given an R-vector F_r, DFFTCF returns in an R-vector I_s

$$I_s = \sum_{r=1}^{R} F_r e^{-2\pi i(r-1)(s-1)/R}, \qquad \text{for } s = 1, \ldots, R. \quad (37)$$

Using this transformation for the terms under the summation operator in (37), $I(d)$ can be written as

$$I(d) = h_x^2 e^{jKd} \Delta\{I_s\} \quad (38)$$

where $\{I_s\}$ is the set of spatial-domain representation of F_r. Note that $\{I_s\}$ is given for the distances of $d_s = 2\pi(s-1)/(2K)$ for $s = 1, \ldots, R$, and this set of distances at which $\{I_s\}$ is calculated is fixed by the sampling frequency of the FFT algorithm $2K/R$. However, these distances, in general, may not correspond to the distances between the basis and testing functions, which are given by $d = (m-n)h_x$ and, consequently, $I(d)$ at the discrete points of d_s are not the MoM matrix entries. Since $I(d = (m-n)h_x)$ is a function of the distance between basis and testing functions, it would be enough to find $I(d = (l-1)h_x)$ for $l = 1, \ldots, N_{te}$. Hence,

$$I(d = (l-1)h_x; l = 1, \ldots, N_{te}) = h_x^2 e^{jK(l-1)h_x} \Delta\{I_s\}, \qquad \text{for } s = \frac{(l-1)Kh_x}{\pi} + 1 \quad (39)$$

is the MoM matrix entries. It is obvious that one application of an FFT algorithm yields all of the MoM matrix entries, resulting in a very efficient approach. Although, this is seemingly the best approach to analyze 2-D problems, the method that is proposed in the following section results in a far more efficient approach and yet is a very suitable one for the optimization problems.

2) Evaluation of MoM Matrix Entries via the GPOF Method: In this section, a novel approach based on the spectral-domain MoM for EFIE for the characterization of 2-D geometries in multilayer media is proposed, and its formulation is given in detail. As for the evaluation of the MoM matrix entries via an FFT algorithm, this approach starts with the EFIE in the spectral domain and then implements the MoM procedure to transform the integral equation into the matrix equation. Therefore, the matrix entries used for this approach are the same as those used for the FFT approach [see (30) and (32)]. The MoM matrix entries, which are single integrals over an infinite domain, can be cast into close forms with the help of the GPOF method. It is not that each entry can be represented by a different closed-form expression, but that there is one closed-form expression valid for all entries. This is achieved by approximating the whole integrand of the MoM matrix entry [see (30) and (32)], except for the exponential term, in terms of complex exponentials, and by getting the inverse Fourier transform of the resulting terms analytically. Remember that the GPOF method is a technique to approximate a function, or a data, by a set of complex exponentials, and it was used for the derivation of the closed-form spatial-domain Green's functions in Section II. Therefore, there is no need for further discussion on the GPOF method, instead, the procedure for the evaluation of the MoM matrix entries is demonstrated for the case of TE excitation, for which a general matrix entry is repeated here, from (30), as follows:

$$\left\langle \tilde{T}_{xm}^{*}, \tilde{G}_{xx}^{E} \tilde{B}_{xn} \right\rangle = \int_{-\infty}^{\infty} dk_x e^{-jk_x h_x (m-n)} h_x^2 \operatorname{sinc}^4\left(\frac{k_x h_x}{2}\right) \tilde{G}_{xx}^{E}$$

where

$$\tilde{G}_{xx}^{E} = \tilde{G}_{xx}^{A} - \frac{k_x^2}{\omega^2} \tilde{G}_{x}^{q_e}$$

$$\begin{aligned} \tilde{G}_{xx}^{E} = {} & \frac{\mu_i k_{z_i}}{j2k_i^2} \Big\{ e^{-jk_{z_i}|z-z'|} - M_i^{\mathrm{TM}} \tilde{R}_{\mathrm{TM}}^{i,i+1} \\ & \cdot e^{-jk_{z_i} 2d_i} e^{jk_{z_i}(z+z')} + M_i^{\mathrm{TM}} \tilde{R}_{\mathrm{TM}}^{i,i-1} \tilde{R}_{\mathrm{TM}}^{i,i+1} \\ & \cdot e^{-jk_{z_i} 2d_i} e^{jk_{z_i}(z-z')} - M_i^{\mathrm{TM}} \tilde{R}_{\mathrm{TM}}^{i,i-1} e^{-jk_{z_i}(z+z')} \\ & + M_i^{\mathrm{TM}} \tilde{R}_{\mathrm{TM}}^{i,i-1} \tilde{R}_{\mathrm{TM}}^{i,i+1} e^{-jk_{z_i} 2d_i} e^{-jk_{z_i}(z-z')} \Big\} \end{aligned} \quad (40)$$

$$= A_0 e^{-jk_{z_i}|z-z'|} + A_1 e^{jk_{z_i}(z+z')} + A_2 e^{jk_{z_i}(z-z')} + A_3 e^{-jk_{z_i}(z+z')} + A_2 e^{-jk_{z_i}(z-z')}. \quad (41)$$

Defining a set of new coefficients like

$$A_l' = j2k_{z_i} \operatorname{sinc}^4\left(\frac{k_x h_x}{2}\right) A_l, \qquad \text{for } l = 0, \ldots, 3. \quad (42)$$

Equation (31) can be written as

$$\begin{aligned} \left\langle \tilde{T}_{xm}^{*}, \tilde{G}_{xx}^{E} \tilde{B}_{xn} \right\rangle = {} & \int_{-\infty}^{\infty} dk_x e^{-jk_x h_x (m-n)} \frac{h_x^2}{j2k_{z_i}} \\ & \cdot \Big\{ A_0' e^{-jk_{z_i}|z-z'|} + A_1' e^{jk_{z_i}(z+z')} + A_2' e^{jk_{z_i}(z-z')} \\ & + A_3' e^{-jk_{z_i}(z+z')} + A_2' e^{-jk_{z_i}(z-z')} \Big\} \end{aligned} \quad (43)$$

where A_l''s are approximated in terms of complex exponentials. Hence, the matrix entries are evaluated analytically, by using the integral identity (5), as

$$\begin{aligned} -jw \left\langle \tilde{T}_{xn}^{*}, \tilde{G}_{xx}^{E} \tilde{B}_{xm} \right\rangle = {} & -\frac{\omega\pi h_x^2}{2} \Bigg\{ \sum_{p_{xx}=1}^{P_{xx}} C_{p_{xx}} H_0^{(2)}(k_i \rho_{p_{xx}}) \\ & + \sum_{p_{1xx}=1}^{P_{1xx}} C_{p_{1xx}} H_0^{(2)}(k_i \rho_{p_{1xx}}) \\ & + \sum_{p_{2xx}=1}^{P_{2xx}} C_{p_{2xx}} H_0^{(2)}\left(k_i \rho_{p_{2xx}}^{(1)}\right) \\ & + \sum_{p_{3xx}=1}^{P_{3xx}} C_{p_{3xx}} H_0^{(2)}(k_i \rho_{p_{3xx}}) \\ & + \sum_{p_{2xx}=1}^{P_{2xx}} C_{p_{2xx}} H_0^{(2)}\left(k_i \rho_{p_{2xx}}^{(2)}\right) \Bigg\} \end{aligned} \quad (44)$$

where

$$\rho_{p_{xx}} = \sqrt{\left[(m-n)h_x\right]^2 + \left(|z-z'| - j\alpha_{p_{xx}}\right)^2}$$
$$\rho_{p_{1xx}} = \sqrt{\left[(m-n)h_x\right]^2 + \left(z+z' + j\alpha_{p_{1xx}}\right)^2}$$
$$\rho^{(1)}_{p_{2xx}} = \sqrt{\left[(m-n)h_x\right]^2 + \left(z-z' + j\alpha_{p_{2xx}}\right)^2}$$
$$\rho^{(2)}_{p_{2xx}} = \sqrt{\left[(m-n)h_x\right]^2 + \left(z-z' - j\alpha_{p_{2xx}}\right)^2}$$
$$\rho_{p_{3xx}} = \sqrt{\left[(m-n)h_x\right]^2 + \left(z+z' - j\alpha_{p_{3xx}}\right)^2}.$$

It is worth mentioning that, since the terms A_l''s are independent of m and n, they are approximated only once and all the elements of the impedance matrix are obtained from the same closed-form representation (44). In addition, since (44) has m, n, z,and z' explicitly, adding new strips or extending the sizes of the strips do not require any further manipulations, one just needs to evaluate (44) for different m, n, z, and z' values.

IV. Results and Discussions

In this section, some results obtained using the three approaches described in the previous section, namely, the spatial-domain MoM with the closed-form Green's functions (spatial), spectral-domain MoM with FFT algorithm (FFT), and spectral-domain MoM with the GPOF method (spectral), are given and discussed. The terms in the parenthesis are used to denote these approaches in the legends of the figures. Note that, for the sake of consistency and brevity, examples of the current densities provided in this paper are selected for the incidence angle of 0°.

Since the numerical efficiency of the spectral-domain MoM in conjunction with the GPOF method is the major issue of this paper, the method of assessment of the efficiency needs to be defined explicitly to show that no bias has been given in favor of this approach. The assessment of the computational efficiency is performed by comparing the CPU times of these three approaches for the same problem as follows: first, the current densities are obtained from the spatial and spectral approaches using the same number of basis functions, and then, the current density for the same geometry is obtained via the FFT-based algorithm with an increasing number of samples for the FFT application until the relative error between the result of the FFT-based approach and those from the other approaches becomes less than some predefined value. For the definition of the relative error, l_2 norm of the difference vector, defined between the vectors consisting of the amplitudes of the basis functions of the current densities obtained by any two of these approaches, has been employed. It is obvious that such comparison favors the FFT-based algorithm because the number of samples is kept at minimum that would satisfy the relative error criterion. Furthermore, this tuning of the number of samples for the FFT-based algorithm to achieve the best performance has been the revelation of another disadvantage of the algorithm.

These techniques are first applied to a single horizontal strip located near the interface of two semiinfinite half-spaces (Fig. 4) for which the presented formulations of these methods in the previous section were based upon. The following parameters are chosen for this example, just to be able to compare the results to those found in the literature [26]–[28] as $\epsilon_{r_i} = 1$ and $\epsilon_{r_{i-1}} = 4$ for the dielectric constants, $2w = 4\lambda_i$ for the width of the strip, and $h = 0$ for the distance of the strip from the interface. The current densities on the strip for TE and TM excitations are obtained by using the three approaches, and are presented in Figs. 5 and 6.

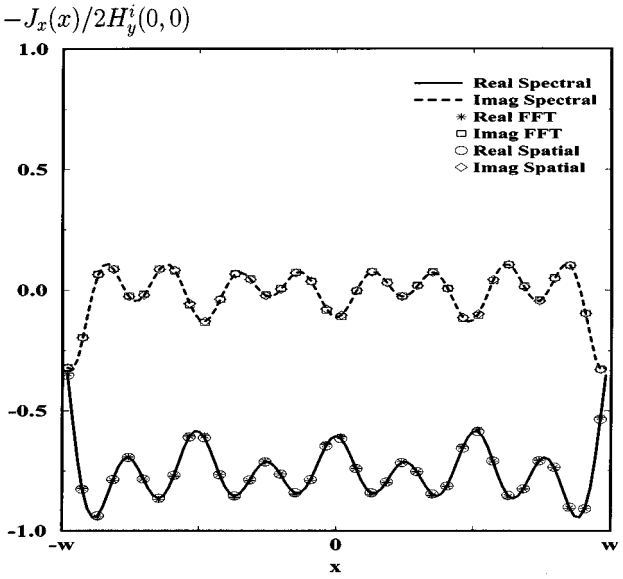

Fig. 5. Real and imaginary parts of the normalized current densities for TE excitation. $\epsilon_{r_{i-1}} = 4.0$, $\epsilon_{r_i} = 1.0$, $2w = 4\lambda_i$, $h = 0$, $\theta = 0^o$.

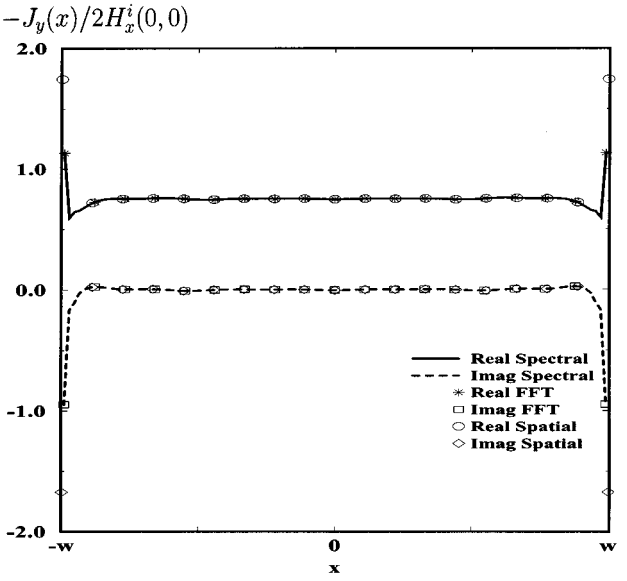

Fig. 6. Real and imaginary parts of the normalized current densities for TM excitation. $\epsilon_{r_{i-1}} = 4.0$, $\epsilon_{r_i} = 1.0$, $2w = 4\lambda_i$, $h = 0$, $\theta = 0^o$.

The results are compared to those provided in [26] and found to be in excellent agreement. The number of basis functions is chosen to be 107 for TE and 109 for TM excitations for both spatial and spectral approaches. Table I shows the CPU times of the three approaches for both TE and TM excitations, and for different angles of incidence. As a result, the spectral-domain MoM with the GPOF method for all the cases has been the most efficient approach.

TABLE I
CPU TIMES OF THE SPECTRAL-DOMAIN, SPATIAL-DOMAIN, AND FFT APPROACHES FOR TE AND TM EXCITATIONS

	CPU time (s)			
	TE		TM	
	$\theta = 0^o$	$\theta = -45^o$	$\theta = 0^o$	$\theta = -45^o$
Spectral	13.7	16.8	10.1	9.8
FFT	16.3	33.0	14.9	15.0
Spatial	361.7	416.5	107.5	108.2

TABLE II
CPU TIMES OF THE SPECTRAL-DOMAIN, SPATIAL-DOMAIN, AND FFT APPROACHES FOR: (a) TE EXCITATION AND (b) TM EXCITATION

	CPU time (s)		
	$h = -0.1\lambda_0$	$h = -0.2\lambda_0$	$h = -0.3\lambda_0$
Spectral	10.5	9.7	9.7
FFT	26.5	54.9	53.7
Spatial	125.5	124.6	124.1

(a)

	CPU time (s)		
	$h = -0.1\lambda_0$	$h = -0.2\lambda_0$	$h = -0.3\lambda_0$
Spectral	11.4	11.2	11.6
FFT	25.0	24.4	24.4
Spatial	39.6	39.3	39.4

(b)

For the second example, the same geometry as in Fig. 4 (with the strip in the dielectric layer $i-1$) is considered to show that the approaches are general, as well as the conclusions. The parameters of the geometry are as follows: $\epsilon_{r_i} = 1$ and $\epsilon_{r_{i-1}} = 4$, $2w = \lambda_{i-1}$, $h = -0.1\lambda_{i-1}, -0.2\lambda_{i-1}$, and $-0.3\lambda_{i-1}$, meaning that the strip is in the lower layer, and $\theta = 0^o$. For this example, the current densities are obtained for both TE and TM excitations for three different values of h, and compared to the results of [27] and [28]. Excellent agreement is again observed between the current distributions obtained by this study and found in the literature, except for a slight deviation near the edges for TM excitations, which might be due to the difference in number and form of the basis functions used in this study and in the study of the references. The number of basis functions is 55 for the TE case and 57 for the TM case. Table II shows the CPU times of the spectral- and spatial-domain approaches and the FFT approach for the TE and TM excitations. Again, the spectral-domain approach uses less computation time as compared to the other approaches.

The geometry of the next example is given in Fig. 7, where Medium 0 is the perfect electric conductor (PEC), $\epsilon_{r_1} = 4$ and $\epsilon_{r_2} = 1$, the width of the strips $2w = 0.5\lambda_2$, and $h_1 = h_2 = \lambda_2$. The number of basis functions is chosen to be 110 for the TE case and 114 for the TM case, and the angle of incidence $\theta = 0^o$.

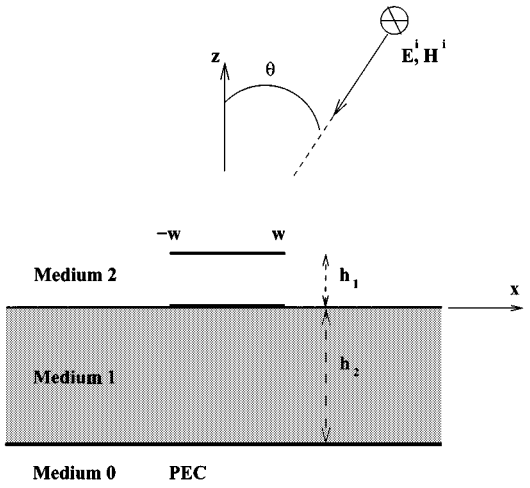

Fig. 7. Two-strip three-layer geometry.

TABLE III
CPU TIMES OF THE SPECTRAL-DOMAIN, SPATIAL-DOMAIN, AND FFT APPROACHES FOR TE AND TM EXCITATIONS

	CPU time (s)	
	TE	TM
Spectral	109.2	63.6
FFT	142.2	166.5
Spatial	6980.2	2187.1

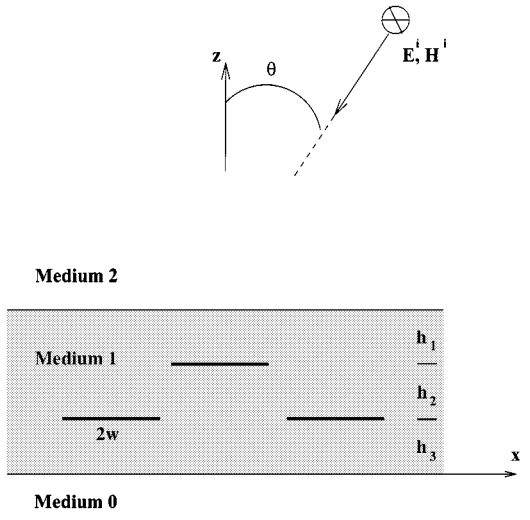

Fig. 8. Three-strip three-layer geometry.

Table III shows the CPU times of all methods for the TE and TM excitations and, again, the CPU time of the spectral-domain approach is the lowest.

After having established the superiority of the GPOF-based technique over the other two techniques for planar geometries in multilayer media, the next example, which is a three-strip geometry in a three-layer medium, is investigated by this approach only. The geometry of the example is given in Fig. 8, where the angle of incidence $\theta = 0^o$, Medium 0, and Medium 2 are free space, $\epsilon_{r_1} = 4$, the width of the strips, $2w = 0.2\lambda_2$, and $h_1 = h_2 = h_3 = 0.1\lambda_2$. The number of basis functions is

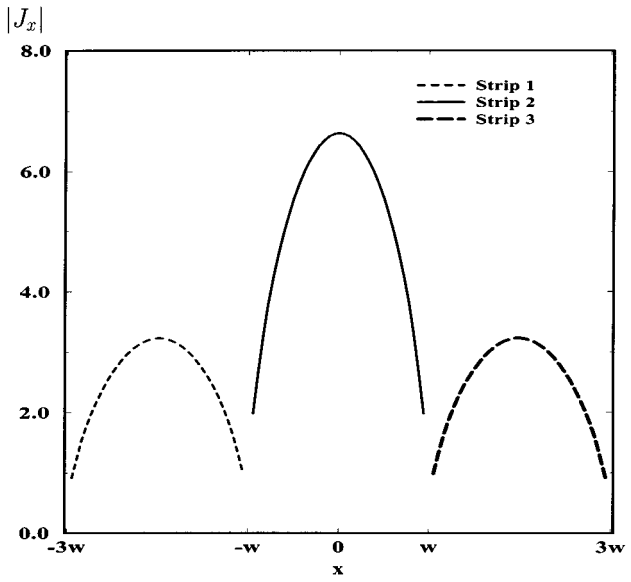

Fig. 9. Magnitudes of the current densities on the three strips for TE excitation. $\epsilon_{r_0} = \epsilon_{r_2} = 1.0, \epsilon_{r_1} = 4, 2w = 0.2\lambda_2, h_1 = h_2 = 0.1\lambda_2, \theta = 0^o$.

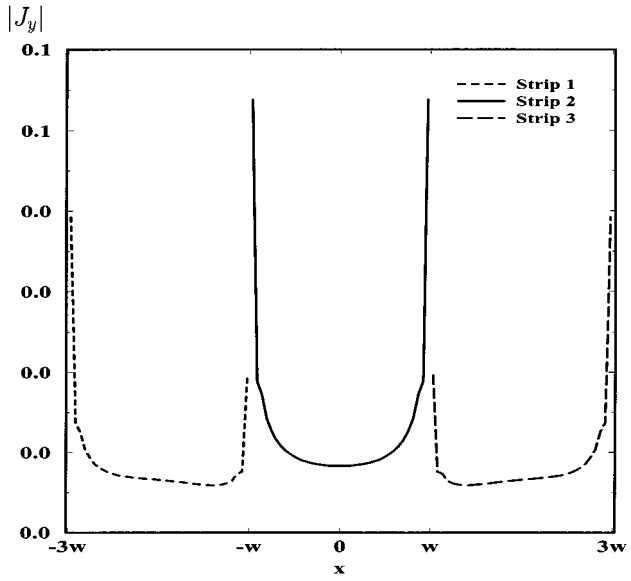

Fig. 10. Magnitudes of the current densities on the three strips for TM excitation. $\epsilon_{r_0} = \epsilon_{r_2} = 1.0, \epsilon_{r_1} = 4, 2w = 0.2\lambda_2, h_1 = h_2 = 0.1\lambda_2, \theta = 0^o$.

chosen to be 105 for the TE case and 111 for the TM case. The CPU time to fill the impedance matrix and the source vector is 106.4 s for the TE case and 71.9 s for the TM case. The magnitudes of the current densities on the strips are given in Figs. 9 and 10 for the TE and TM excitations, respectively.

V. Conclusion

As it is well known, the application of the MoM to 2-D planar multilayer geometries transforms integral equations into matrix equations whose entries are double integrals over finite domains in the spatial-domain MoM, and single integrals over infinite domain in the spectral-domain MoM. In this paper, three different algorithms to efficiently evaluate those integrals have been studied, which are: 1) the use of closed-form Green's functions for the spatial-domain MoM formulation; 2) the use of the GPOF; and 3) the use of the FFT algorithm, both in the spectral-domain MoM formulation. The first two approaches have been developed in this paper and the results obtained for different applications are compared with each other and with the third approach. It is observed that there is no accuracy problem in any of these approaches, but as far as the numerical efficiency of these algorithms are concerned, the one using the GPOF formulation is the best, which has been verified for several examples by giving the CPU times for filling the MoM matrices.

References

[1] R. F. Harrington, "Matrix methods for field problems," *Proc. IEEE*, vol. 55, pp. 136–149, Feb. 1967.

[2] ——, *Field Computation by Moment Methods*. New York: Macmillan, 1983.

[3] J. Jin, *The Finite Element Method in Electromagnetics*. New York: Wiley, 1993.

[4] K. Kunz and R. Luebber, *The Finite Difference Time Domain Method for Electromagnetics*. Boca Raton, FL: CRC Press, 1993.

[5] J. L. Tsalamengas, "Direct singular equation methods in scattering and propagation in strip- or slot-loaded structures," *IEEE Trans. Antennas Propagat.*, vol. 46, pp. 1560–1570, Oct. 1998.

[6] ——, "Scattering of arbitrarily polarized plane waves obliquely incident on infinite slots or strips in a planar-stratified medium," *IEEE Trans. Antennas Propagat.*, vol. 46, pp. 1634–1640, Nov. 1998.

[7] ——, "Exponentially converging direct singular integral-equation methods in the analysis of microslot lines on layered substrates," *IEEE Trans. Microwave Theory Tech.*, vol. 47, pp. 2031–2034, Oct. 1999.

[8] J. Bernal, F. Medina, R. R. Boix, and M. Horno, "Fast full-wave analysis of multistrip transmission lines based on MPIE and complex image theory," *IEEE Trans. Microwave Theory Tech.*, vol. 48, pp. 445–452, Mar. 2000.

[9] L. Gurel and W. C. Chew, "A recursive T-matrix algorithm for strips and patches," *Radio Sci.*, vol. 27, pp. 387–401, May–June 1992.

[10] J. T. Fessler, K. W. Whites, and C. R. Paul, "The effectiveness of an image plane in reducing radiated emissions," *IEEE Trans. Electromagn. Compat.*, vol. 38, pp. 51–61, Feb. 1996.

[11] J. R. Mosig, "Arbitrarily shaped microstrip structures and their analysis with a mixed potential integral equation," *IEEE Trans. Microwave Theory Tech.*, vol. 36, pp. 314–323, Feb. 1988.

[12] L. Alatan, M. I. Aksun, K. Mahadevan, and M. T. Birand, "Analytical evaluation of the MoM matrix elements," *IEEE Trans. Microwave Theory Tech.*, vol. 44, pp. 519–525, Apr. 1996.

[13] A. Taflove, "State of the art and future directions in finite-difference and related techniques in supercomputing computational electromagnetics," in *Directions in Electromagnetic Wave Modeling*, H. L. Bertoni and L. B. Felsen, Eds. New York: Plenum, 1991.

[14] D. G. Fang, J. J. Yang, and G. Y. Delisle, "Discrete image theory for horizontal electric dipoles in a multilayered medium," *Proc. Inst. Elect. Eng.*, pt. H, vol. 135, pp. 297–303, Oct. 1988.

[15] Y. L. Chow, J. J. Yang, D. F. Fang, and G. E. Howard, "A closed-form spatial Green's function for the thick microstrip substrate," *IEEE Trans. Microwave Theory Tech.*, vol. 39, pp. 588–592, Mar. 1991.

[16] M. I. Aksun and R. Mittra, "Derivation of closed-form Green's functions for a general microstrip geometries," *IEEE Trans. Microwave Theory Tech.*, vol. 40, pp. 2055–2062, Nov. 1992.

[17] G. Dural and M. I. Aksun, "Closed-form Green's functions for general sources and stratified media," *IEEE Trans. Microwave Theory Tech.*, vol. 43, pp. 1545–1552, July 1995.

[18] N. Kinayman and M. I. Aksun, "Efficient use of closed-form Green's functions for the analysis of planar geometries with vertical connections," *IEEE Trans. Microwave Theory Tech.*, vol. 45, pp. 593–603, May 1997.

[19] ——, "Efficient and accurate EM simulation technique for analysis and design of MMICs," *Int. J. Microwave Millimeter-Wave Computer-Aided Eng.*, vol. 7, pp. 344–358, Sept. 1997.

[20] ——, "Efficient evaluation of the MoM matrix entries for planar geometries in multilayer media," *IEEE Trans. Microwave Theory Tech.*, vol. 48, pp. 309–312, Feb. 2000.

[21] Y. Hua and T. K. Sarkar, "Generalized pencil-of-function method for extracting poles of an EM system from its transient response," *IEEE Trans. Antennas Propagat.*, vol. 37, pp. 229–234, Feb. 1989.

[22] W. C. Chew, *Waves and Fields in Inhomogeneous Media*. New York: Van Nostrand, 1990.
[23] N. K. Das and D. M. Pozar, "A spectral-domain Green's function for multilayer dielectric substrates with application to multilayer transmission lines," *IEEE Trans. Microwave Theory Tech.*, vol. MTT-35, pp. 326–335, Mar. 1987.
[24] M. I. Aksun, "A robust approach for the derivation of the closed-form Green's functions," *IEEE Trans. Microwave Theory Tech.*, vol. 44, pp. 651–658, May 1996.
[25] M. I. Aksun and R. Mittra, "Choices of expansion and testing functions for the method of moments applied to a class of electromagnetic problems," *IEEE Trans. Microwave Theory Tech.*, vol. 41, pp. 503–509, Mar. 1993.
[26] C. M. Butler, "Current induced on a conducting strip which resides on the planar interface between two semi-infinite half-spaces," *IEEE Trans. Antennas Propagat.*, vol. AP-32, pp. 226–231, Mar. 1984.
[27] X.-B. Xu, C. M. Butler, and A. W. Glisson, "Current induced on a conducting cylinder located near the planar interface between two semi-infinite half-spaces," *IEEE Trans. Antennas Propagat.*, vol. AP-33, pp. 616–624, June 1985.
[28] X.-B. Xu and C. M. Butler, "Current induced by TE excitation on a conducting cylinder located near the planar interface between two semi-infinite half-spaces," *IEEE Trans. Antennas Propagat.*, vol. AP-34, pp. 880–890, July 1986.

M. I. Aksun (M'92–SM'99) received the B.S. and M.S. degrees in electrical and electronics engineering from the Middle East Technical University, Ankara, Turkey, in 1981 and 1983, respectively, and the Ph.D. degree in electrical and computer engineering from the University of Illinois at Urbana-Champaign (UIUC), in 1990.

From 1990 to 1992, he was a Post-Doctoral Fellow in the Electromagnetic Communication Laboratory, UIUC. From 1992 to 2001, he was on the faculty of the Department of Electrical and Electronics Engineering, Bilkent University, Ankara, Turkey, where, since 1999, he was a Professor. In 2001, he has joined the Department of Electrical and Electronics Engineering, Koç University, Istanbul, Turkey, where he is currently a Professor. His research interests include numerical methods for electromagnetics, microstrip antennas, indoor and outdoor propagation models, and microwave and millimeter-wave integrated circuits.

F. Çalışkan (S'99), photograph and biography not available at time of publication.

Levent Gürel (S'88–M'91–SM'97) was born in İzmir, Turkey, in 1964. He received the B.Sc. degree from the Middle East Technical University (METU), Ankara, Turkey, in 1986, and the M.S. and Ph.D. degrees from the University of Illinois at Urbana-Champaign (UIUC), in 1988 and 1991, respectively, all in electrical engineering.

In 1991, he joined the Thomas J. Watson Research Center, IBM Corporation, Yorktown Heights, NY, where he was a Research Staff Member involved with the electromagnetic compatibility (EMC) problems related to electronic packaging, the use of microwave processes in the manufacturing and testing of electronic circuits, and the development of fast solvers for interconnect modeling. In 1993, he was awarded the title of Associate Professor by the Institute of Higher Education, Ankara, Turkey. Since 1994, he has been a faculty member in the Department of Electrical and Electronics Engineering, Bilkent University, Ankara, Turkey. He was a Visiting Associate Professor at the Center for Computational Electromagnetics (CCEM), UIUC, for one semester in 1997. He has authored or co-authored several papers in IEEE publications. His research interests include the development of fast algorithms for computational electromagnetics (CEM) and the application thereof to scattering and radiation problems involving large and complicated scatterers, antennas and radars, frequency-selective surfaces, and high-speed electronic circuits. He is also interested in the theoretical and computational aspects of electromagnetic compatibility and interference analyses and ground-penetrating radars and other subsurface-scattering applications.

Dr. Gürel is currently the chairman of the IEEE Antennas and Propagation Society (IEEE AP-S)/IEEE Microwave Theory and Techniques Society (IEEE MTT-S)/IEEE Electron Devices Society (IEEE ED-S)/IEEE Electromagnetic Compatibility Society (IEEE EMC-S) Chapter of the IEEE Turkey Section. Since 1987, he has attended numerous IEEE International Symposia and has served as a reviewer for various IEEE publications.